JOURNAL OF Materials CHEMISTRY

Second-order non linear optical properties of nitrocalixarenes grafted to a sol-gel matrix

Mourad Regayeg,[a] Alain Fort,[b] Olivier Cregut,[b] Anthony Coleman,[c] Patrick Shahgaldian,[c] Jacques Mugnier,[d] Roger Lamartine[a] and Francis Vocanson*[a]

[a]*SROMB, UMR 5078 CNRS, Université Lyon I, 43 boulevard du 11 novembre 1918, 69622 Villeurbanne Cédex, France. E-mail: f.vocanson@cdlyon.univ-lyon1.fr; Fax: 33 4 72 44 84 38; Tel: 33 4 72 44 80 14*
[b]*IPCMS-GONLO, UMR 7504 CNRS, 23 rue du Loess, 67037 Strasbourg Cedex, France*
[c]*IBCP, Université Lyon I, UMR 5086 CNRS, 7 passage du Vercors, 69367 Lyon Cédex 07, France*
[d]*LPCML, UMR 5620 CNRS, Université Lyon I, 43 boulevard du 11 novembre 1918, 69622 Villeurbanne Cédex, France*

Received 28th February 2002, Accepted 26th April 2002
First published as an Advance Article on the web 13th June 2002

5,11,17,23-Tetranitro-25-[4-[3-(trimethoxysilyl)propylthio]-butyloxy]-26,27,28-tripropyloxycalix[4]arene was prepared and fully characterized using ^{1}H and ^{13}C NMR. Elaboration of sol-gel matrix with this macrocycle and with tetranitrotetrapropoxycalix[4]arene from tetraethoxysilane was described. Thin films were obtained from these materials and studied using m-lines spectroscopy, AFM and NLO. Chemically grafted films exhibited high and stable NLO responses.

1 Introduction

One of the major goals in the development of opto-electronic materials lies in the production of systems exhibiting high second-order susceptibilities, and that also possess excellent temporal, physical and chemical stabilities, over time, for use in optical switching, frequency switching, and data storage.[1] Until recently, non-centrosymmetric crystals including organic material such as urea or inorganic materials such as quartz or lithium niobate, have been the most widely used media.[2] However hybrid organic–inorganic sol-gels represent a promising alternative; they can be cast as films and molecular orientation within the sol-gel framework is possible by use of corona poling.[3] Furthermore they may be processed by techniques such as thermal imprinting to yield microstructured materials such as optical waveguides.[4]

Calixarenes, widely studied for their host–guest properties, present thermally and physically robust structures based on phenolic methylene bridged macrocycles.[5] They are simple and cheap to produce, and their chemical derivation has been broadly developed.[5] The use of the nitrocalix[4]arenes as non linear optical (NLO) materials has been studied by Reinhoudt in solution,[6] in thin films[6] and in grafted polymer systems.[7] Good second order NLO properties have been observed for these materials. However, in the case of the *p*-nitrocalix[4]-arenes thin films, there was a strong and rapid decrease in the NLO properties[6] over time. This could be avoided using grafted polymer systems,[7] however the stability of such systems with regard to solvents is likely to be low and their thermal stability is restricted to about 150 °C.

More interesting was the demonstration by Reinhoudt of the possibility of using electrical fields to pole the films.[6] We ourselves have observed that spatial orientation of crystallisation in simple calix[4]arene thermally deposited films may be induced by annealing in a magnetic field.

In this paper we describe methods to improve thermal, mechanical and chemical stability of calix[*n*]arene based NLO materials, firstly by simple inclusion of nitrocalix[4]arenes into sol-gels and secondly by chemically coupling the molecules into the sol-gel matrix. It is shown that the chemically grafted nitrocalix[4]arene sol-gels may be prepared as thin films. These thin films show good second-order susceptibilities, coupled with the possibility of planar wave guiding. AFM studies show that in the case of simple inclusion in the sol-gel matrix, there is a dephasing of the components explaining the poor optical behaviour of these materials. However this dephasing is not detected in the case of the chemically grafted materials; the materials present no topographically observable changes induced by the Corona poling process.

2 Experimental

2.1 General

All chemicals were purchased from Aldrich and used without further purification. Melting points were determined with an Electrothermal 9100 melting point apparatus and are uncorrected. ^{1}H and ^{13}C NMR spectra were recorded on a Bruker AM 300 spectrometer in $CDCl_3$ at room temperature with Me_4Si as internal reference and solid state ^{29}Si CP/MAS (cross polarization/magic angle spinning) NMR spectra were recorded on a Bruker DSX 300 MHz spectrometer. Electrospray mass spectra were recorded with a Perkin Elmer SCIEX API 165. UV-visible spectra were recorded with a Shimadzu UV-2401 PC spectrometer. All reactions were carried under a nitrogen atmosphere.

2.2 Synthesis

Tetranitrotetrapropoxycalix[4]arene **1** was synthesized according to the protocol described by Reinhoudt.[8]

p-Tert-butyl-25,26,27-tripropyloxy-28-hydroxycalix[4]arene **2** was synthesized by the procedure described by Wamoto *et al.*[9]

5,11,17,23-Tetra-*tert*-butyl-25-(4-bromobutyloxy)-26,27,28-tripropyloxycalix[4]arene **3**: to a stirred suspension of 0.094 g (at 60% in oil, washed in *n*-hexane, 2.3 mmol) of sodium hydride in 1.3 mL of DMF and 5.2 mL of THF was added 0.13 g (0.1368 mmol) of *p-tert*-butyl-25,26,27-tripropyloxy-28-hydroxycalix[4]arene **2** at room temperature. After 30 min,

DOI: 10.1039/b202131e

0.27 mL (2.3 mmol) of 1,4-dibromobutane was added. The mixture was stirred during 4 hours at 80 °C. After cooling, the solvent was removed by evaporation. 20 mL of H_2O were added. The residue was extracted with $CHCl_3$ (3 × 30 mL) and the combined organic layers were dried over $MgSO_4$ and evaporated. Recrystallization from $CHCl_3$–MeOH afforded pure **3** in 78.5% yield; mp 180 °C; ^{1}H NMR: δ 1.0 (m, 9H, 3 O-CH$_2$-CH$_2$-C*H*$_3$), 1.05 (s, 18H, 2((C*H*$_3$)$_3$C), 1.1 (s, 18H, 2((C*H*$_3$)$_3$C), 2.04 (m, 8H, 3 O-CH$_2$-C*H*$_2$-CH$_3$ and O-CH$_2$-C*H*$_2$-CH$_2$-CH$_2$-Br), 2.14 (m, 2H, -O-CH$_2$-CH$_2$-C*H*$_2$-CH$_2$-Br), 3.12 (d, 4H, *J* = 12.5, Ar-C*H*$_2$-Ar), 3.5 (t, 2H, -O-CH$_2$-CH$_2$-CH$_2$-C*H*$_2$-Br), 3.8 (m, 6H, 3 O-C*H*$_2$-CH$_2$-CH$_3$), 3.89 (t, 2H, *J* = 4.38, O-C*H*$_2$-CH$_2$-CH$_2$-CH$_2$-Br), 4.37 (d; 2H, *J* = 12.5, Ar-C*H*$_2$-Ar), 4.41 (d, 2H, J = 12.5, Ar-C*H*$_2$-Ar), 6.74 (s, 4H, Ar-*H*), 6.81 (s, 4H, Ar-*H*); ^{13}C NMR: δ 10.79 (O-CH$_2$-CH$_2$-*C*H$_3$), 23.81 and 23.68 (O-CH$_2$-*C*H$_2$-CH$_3$), 29.46 (O-CH$_2$-*C*H$_2$-CH$_2$-CH$_2$-Br), 30.22 (O-CH$_2$-CH$_2$-*C*H$_2$-CH$_2$-Br), 31.47 (Ar-*C*H$_2$-Ar: cone conformation), 31.84 and 31.89 ((*C*H$_3$)C), 33.98 (O-CH$_2$-CH$_2$-CH$_2$-*C*H$_2$-Br), 34.19 and 34.24 ((CH$_3$)*C*), 74.49 (O-*C*H$_2$-CH$_2$-CH$_3$), 77.29 (O-*C*H$_2$-CH$_2$-CH$_2$-CH$_2$-Br), 125.19, 125.32 and 125.42 (Ar-*C*H), 133.90, 134.07, 134.33 and 134.44 (Ar-*C*CH$_2$), 144.58, 144.63 and 144.88 (Ar-*C*(CH$_3$)C), 153.93, 153.99 and 154.13 (Ar-*C*O); MS (ES): *m*/*z*: 911.3 [M+H]$^+$, calcd 911; UV/Vis (CH_2Cl_2): λ_{max} = 307 nm (ε = 3980) and 282 nm (ε = 4080).

5,11,17,23-Tetranitro-25-(4-bromobutyloxy)-26,27,28-tripropyloxycalix[4]arene **4**: to a solution of 0.18 g (0.198 mmol) of calixarene **3** in 3 mL of CH_2Cl_2, cooled at 0 °C, were added 3 mL of glacial acetic acid and 1 mL of fuming nitric acid. The mixture was stirred at room temperature until the initial purple-black coloration became yellow. The reaction mixture was also poured onto ice–water and 10 mL of CH_2Cl_2 and 10 mL of H_2O were added. The aqueous layer was extracted twice with 10 mL of CH_2Cl_2, and the combined organic layers were washed with 10 mL of sodium bicarbonate solution and 2 × 20 mL of brine, dried over $MgSO_4$, and evaporated. Recrystallisation from $CHCl_3$–MeOH afforded pure **4** in 74% yield; mp 230 °C; ^{1}H NMR: δ 1.04 (m, 9H, 3 O-CH$_2$-CH$_2$-C*H*$_3$), 1.9 (m, 8H, 3 O-CH$_2$-C*H*$_2$-CH$_3$ and O-CH$_2$-C*H*$_2$-CH$_2$-CH$_2$-Br), 1.93 (m, 2H, O-CH$_2$-CH$_2$-C*H*$_2$-CH$_2$-Br), 3.41 (d, 2H, *J* = 13.98, Ar-C*H*$_2$-Ar), 3.42 (d, 2H, J = 13.98, Ar-C*H*$_2$-Ar), 3.48 (t, 2H, O-CH$_2$-CH$_2$-CH$_2$-C*H*$_2$-Br), 3.9 (m, 8H, 3 O-C*H*$_2$-CH$_2$-CH$_3$ and O-C*H*$_2$-CH$_2$-CH$_2$-CH$_2$-Br), 4.5 (d, 2H, *J* = 13.98, Ar-C*H*$_2$-Ar), 4.52 (d, 2H, *J* = 13.98, Ar-C*H*$_2$-Ar), 7.55 (s, 4H, ArH), 7.61 (s, 4H, ArH); ^{13}C NMR: δ 10.55 and 10.64 (O-CH$_2$-CH$_2$-*C*H$_3$), 23.66 and 23.70 (O-CH$_2$-*C*H$_2$-CH$_3$), 29.19 and 29.53 (O-CH$_2$-*C*H$_2$-CH$_2$-CH$_2$-Br and O-CH$_2$-CH$_2$-*C*H$_2$-CH$_2$-Br), 31.52 (Ar-*C*H$_2$-Ar: cone conformation), 33.31 (O-CH$_2$-CH$_2$-CH$_2$-*C*H$_2$-Br), 75.51 (O-*C*H$_2$-CH$_2$-CH$_3$), 78.17 (O-*C*H$_2$-CH$_2$-CH$_2$-CH$_2$-Br), 124.34 and 124.53 (Ar-*C*H), 135.75 and 135.93 (Ar-*C*CH$_2$), 144.58, 143.25 and 143.39 (Ar-*C*-NO$_2$), 161.73 and 162.14 (Ar-*C*O); MS (ES): *m*/*z*: 867 [M+H]$^+$, calcd 867; UV/Vis (CH_2Cl_2): λ_{max} = 291.5 nm (ε = 31214).

5,11,17,23-Tetranitro-25-[4-[3-(trimethoxysilyl)propylthio]-butyloxy]-26,27,28-tripropyloxycalix[4]arene **5**: to a suspension of 0.2 g (0.23 mmol) of calixarene **4** in 20 mL of THF and 0.124 g (2.3 mmol) of sodium methoxide was added 0.42 mL (2.3 mmol) of 3-mercaptopropyltrimethoxysilane. The mixture was stirred at room temperature during 24 h. After evaporation of solvent, the residue was taken up in 20 mL of $CHCl_3$ and the precipitate was removed by filtration. The solvent was evaporated. Recrystallization from $CHCl_3$–MeOH afforded pure **5** in 77% yield as yellow powder; mp 220 °C; ^{1}H NMR: δ 0.74 (t, 2H, -O-CH$_2$-CH$_2$-CH$_2$-CH$_2$-S-CH$_2$-CH$_2$-C*H*$_2$-Si(OCH$_3$)$_3$), 1.0 (t, 9H, 3 O-CH$_2$-CH$_2$-C*H*$_3$), 1.92 (m, 12H, 3 -O-CH$_2$-C*H*$_2$-CH$_3$, O-CH$_2$-C*H*$_2$-CH$_2$-CH$_2$-S-CH$_2$-CH$_2$-CH$_2$-Si(OCH$_3$)$_3$, O-CH$_2$-CH$_2$-C*H*$_2$-CH$_2$-S-CH$_2$-CH$_2$-CH$_2$-Si(OCH$_3$)$_3$ and O-CH$_2$-CH$_2$-CH$_2$-CH$_2$-S-CH$_2$-C*H*$_2$-CH$_2$-Si(OCH$_3$)$_3$), 2.55 (m, 4H, -O-CH$_2$-CH$_2$-CH$_2$-C*H*$_2$-S-C*H*$_2$-CH$_2$-CH$_2$-Si(OCH$_3$)$_3$), 3.4 (d, 4H, *J* = 13.95, Ar-C*H*$_2$-Ar), 3.56 (s, 9H, O-CH$_2$-C*H*$_2$-CH$_2$-CH$_2$-S-CH$_2$-CH$_2$-CH$_2$-Si(OC*H*$_3$)$_3$), 3.95 (m, 8H, 3 O-C*H*$_2$-CH$_2$-CH$_3$ and O-C*H*$_2$-CH$_2$-CH$_2$-CH$_2$-S-CH$_2$-CH$_2$-CH$_2$-Si(OCH$_3$)$_3$), 4.5 (d, 2H, *J* = 13.95, Ar-C*H*$_2$-Ar), 4.52 (d, 2H, *J* = 13.95, Ar-C*H*$_2$-Ar), 7.56 (s, 4H, ArH), 7.59 (s, 4H, ArH); ^{13}C NMR: δ 9.08 (O-CH$_2$-CH$_2$-CH$_2$-CH$_2$-S-CH$_2$-CH$_2$-*C*H$_2$-Si(OCH$_3$)$_3$), 10.56 (O-CH$_2$-CH$_2$-*C*H$_3$), 23.43 and 23.68 (O-CH$_2$-*C*H$_2$-CH$_3$ and O-CH$_2$-*C*H$_2$-CH$_2$-CH$_2$-S-CH$_2$-CH$_2$-CH$_2$-Si(OCH$_3$)$_3$), 26.35 and 29.67 (O-CH$_2$-CH$_2$-*C*H$_2$-CH$_2$-S-CH$_2$-CH$_2$-CH$_2$-Si(OCH$_3$)$_3$ and O-CH$_2$-CH$_2$-CH$_2$-CH$_2$-S-CH$_2$-*C*H$_2$-CH$_2$-Si(OCH$_3$)$_3$), 31.53 (Ar-*C*H$_2$-Ar: cone conformation), 35.65 (O-CH$_2$-CH$_2$-CH$_2$-*C*H$_2$-S-*C*H$_2$-CH$_2$-CH$_2$-Si(OCH$_3$)$_3$), 50.97 (O-CH$_2$-CH$_2$-CH$_2$-CH$_2$-S-CH$_2$-CH$_2$-CH$_2$-Si(O*C*H$_3$)$_3$), 76.04 (O-*C*H$_2$-CH$_2$-CH$_3$), 78.14 (O-*C*H$_2$-CH$_2$-CH$_2$-CH$_2$-S-CH$_2$-CH$_2$-CH$_2$-Si(OCH$_3$)$_3$), 124.43 (Ar-*C*H), 135.77 and 135.83 (Ar-*C*CH$_2$), 143.28 (Ar *C*-NO$_2$), 162.07 (Ar-CO); MS (ES): m/z: 981 [M+H]$^+$, calcd 980; UV/Vis (CH_2Cl_2): δ_{max} = 293.5 nm (ε = 26160).

2.3 Sol-gel preparation

Class I sol-gel: to a solution of tetranitrotetrapropoxycalix[4]-arene and tetraethoxysilane (TEOS) in acetone was added water (pH = 1); alkoxysilane : water : acetone molar ratios were 1 : 5.5 : 6. After hydrolysis for one hour at room temperature, pyridine was added to the solution with an alkoxysilane : pyridine molar ratio of 0.3. After standing for one hour, the sol was passed through a 0.45 µm filter before deposition. Systems with nitrocalix[4]arene **1** : alkoxysilane 1 : 1 and 1 : 9 molar ratios were prepared by the same method. As the optical quality of these films was unsuitable for planar wave guiding, we have prepared TiO_2 films.[10] To a solution of titanium isopropoxide in isopropyl alcohol was added acetic acid after 10 minutes. Then a solution of nitrocalix[4]-arene **1** in chloroform was added to the initial solution with different concentrations in macrocycle. Titanium isopropoxide : calixarene molar ratios studied were 1 : 80, 1 : 120, 1 : 240. After mixing for one hour and standing for the same time, the sol was passed through a 0.45 µm filter before deposition.

Class II sol-gel: to a solution of nitrocalix[4]arene **5** and TEOS (1 : 39 or 1 : 19 molar ratios) in acetone was added water (pH = 1); alkoxysilane : water : acetone molar ratios were 1 : 2 : 6. After hydrolysis for one hour at room temperature, pyridine was added to the solution with an alkoxysilane : pyridine molar ratio of 0.3. After standing for one hour, the sol was passed through a 0.45 µm filter before deposition.

The measurements of solid state ^{29}Si CP/MAS NMR were performed on the nitrocalix[4]arene **5**–TEOS (1 : 19 molar ratio) gel and on the nitrocalix[4]arene **1**–TEOS (1 : 19 molar ratio) gel.

2.4 Film deposition

Crack-free sol-gel films were deposited from solution *via* spin-coating (spinning rate of 2000 rpm) or dip-coating onto glass substrates for AFM studies, either onto optically polished silica plates (Herasil from Heraeus®) or onto Pyrex® plates for m-lines spectroscopy studies, and onto ITO substrates for NLO studies. All these substrates were previously cleaned with detergent, treated with ultrasonics in acetone, ethanol, deionized water and wiped with lens cleaning tissue.

For NLO studies the neat films deposited by spin-coating were oriented at 120 °C for 3 hours by Corona poling with a tungsten wire located at a distance of 20 mm from the film and elevated at a 3 kV voltage. The experiments were immediately realized after poling or one day later. The results were similar in the two cases.

2.5 Wave guide studies

The refractive indices of the films at a wavelength of 543.5 nm (He-Ne laser) and their thickness were calculated by measuring the angle for frustrated reflection in the film for light coupled through a high index prism, using m-lines spectroscopy.[11] For that purpose, an isosceles LaSF35 (Schott) glass prism is squeezed against the sample (*i.e.* the film on its substrate). The assembly is mounted in a controlled rotary stage with an angular resolution of 0.001°. Depending on incident polarisation being either TE (Transverse Electric) or TM (Transverse Magnetic), there are dips in reflection at angular positions corresponding to the excitation of guiding modes. We measured the angular position of these dips. Two TE and two TM modes are required to obtain accuracy for either the refractive index or the thickness of the studied film. Note that if the film supports only one TE and one TM mode it is also possible to obtain these optogeometric parameters (thickness and refractive index respectively) but the resultant accuracy is much reduced.

2.6 AFM studies

Atomic Force Microscopy was carried out in air, in the contact mode using a Topometrix Explorer AFM with a 100 µm scanner. Scan rates were typically 1.5 Hz. Data were collected in the topographic, lateral force and force modulation modes. The samples used in the NLO experiments were studied after poling using both contact and non-contact modes. Images were collected from 100 µm to 5 µm scan ranges. The images presented are unfiltered. Roughness and object analysis were carried out using the Thermomicroscopes SMPL 4.0 and SMPL 5.01 software packages.

2.7 Non linear optical properties

The determination of the optical non linearities was performed by measurement of second harmonic light generated by an incident laser beam illuminating the samples. The conventional EFISH[12,13] set-up was used to measure the quadratic hyperpolarizability β of the molecules in solution, while the MAKER fringe technique[12] was chosen for the evaluation of the quadratic susceptibility of the films. The light source was a Nd:YAG laser emitting at a wavelength of 1.064 µm.

In the case of EFISH measurements the polarization was set parallel to the vertical electric field applied to the molecules, and the initial wavelength of the laser was Raman shifted to 1.907 µm by using a high pressure hydrogen cell. In these conditions, there is no absorption at the fundamental and harmonic wavelengths, allowing a simplified analysis of the results (Kleinmann symmetry conditions). Neglecting the non orientational term, the technique determines the product $\mu_g\beta(2\omega)$ where μ_g represents the permanent fundamental dipole moment and $\beta(2\omega)$ the quadratic hyperpolarizability at the harmonic laser pulsation 2ω. For a rod shaped molecule, $\beta(2\omega)$ is one dimensional along the charge transfer (CT) axis of the molecule. In the case of calixarenes, the component along the cone axis is predominant. In the two level approximation, the static quadratic hyperpolarizability $\beta(0)$ is then deduced from a simple dispersion relation:

$$\beta(2\omega)=\beta(0)\frac{\omega_{\mathrm{CT}}^4}{(\omega_{\mathrm{CT}}^2-4\omega^2)(\omega_{\mathrm{CT}}^2-\omega^2)}$$

$$\beta(0)=\frac{3\mu_{\mathrm{eg}}^2(\mu_{\mathrm{e}}-\mu_{\mathrm{g}})}{2\hbar\omega_{\mathrm{CT}}^2}$$

where $\nabla\omega_{\mathrm{CT}}$ corresponds to the transition energy to the first excited CT state, μ_{eg} to the electric dipole transition matrix element between the fundamental and the CT state and μ_{e} to the dipole moment of the excited state. The signals of second harmonic generation (SHG) were calibrated relative to quartz whose susceptibility $d_{11} = 1.2\ 10^{-19}$ esu at 1.064 µm was extrapolated to the value 1.1 10^{-19} esu at 1.907 µm.

For the determination of the non linearities of the films, the usual quartz wedge used for EFISH fringes calibration was replaced by a quartz crystal oriented with the *z* axis taken as the rotation axis, the incident *s* polarization of the beam laying in the ordinary plane. In this configuration, the only relevant term is d_{11}[14] and the amplitude of the SHG signal is proportional to[14]

$$\mathrm{d}^2\mathrm{Tr}_{2\omega}.\mathrm{Tr}_{\omega}^4.\sin(\Psi)^2/(\mathrm{no}_{\omega}^2-\mathrm{no}_{2\omega}^2)^2$$

where d is the effective nonlinear coefficient taking into account the geometry of the experiment ($d = d_{11}\cos(3.\theta_\omega)$), $\mathrm{Tr}_{2\omega}$ and Tr_ω are the transmission coefficients respectively for the harmonic and fundamental field. The angle

$$\Psi=(\pi.L).2/\lambda.(\mathrm{no}_\omega\cos(\theta_\omega)-\mathrm{no}_{2\omega}\cos(\theta_{2\omega}))$$

corresponds to the dephasing between the free wave and the bound wave.

In our experiments, the geometry remains the same for all the samples. The group of symmetry of the sample leads to an effective nonlinear coefficient expressed as:

$$d=d_{33}((\sin(\theta_\omega))^2+\mathrm{xalpha}.\cos(\theta_\omega)^2).\sin(\theta_{2\omega})$$
$$+\,\mathrm{xalpha}.\sin(2\theta_\omega).\cos(\theta_{2\omega}))$$

The SHG signal is proportional to

$$\mathrm{d}^2\mathrm{Tr}_{2\omega}.\mathrm{Tr}_{\omega}^4.\sin(\Psi)^2/(n_{\omega}^2-n_{2\omega}^2)^2$$

However, due to the low thickness of the samples, this expression can be simply written as:

$$\mathrm{d}^2.\mathrm{Tr}_{\omega}^4.\mathrm{Tr}_{2\omega}.(\pi L)^2/(\lambda.n_\omega.\cos(\theta_{2\omega}))^2$$

i.e. an expression independent of the precise knowledge of the index dispersion.

3 Results and discussion

The synthesis of tetranitrotetrapropoxycalix[4]arene **1** (Fig. 1) is already described[8] and the compound is obtained with a good yield. It is also an interesting compound because of its high solubility in organic solvent. The synthetic route to a modified nitrocalix[4]arene is depicted in Fig. 2. The resulting nitrocalix[4]arene **5** was stable at 10 °C under nitrogen and anhydrous conditions.

The sol-gel process allows the synthesis of new hybrid organic–inorganic compounds.[3,15] The properties of these materials depend on components and on the interface between these phases. According to Sanchez and Lebeau,[3] hybrid materials can be divided into two classes:

Class I which involves organic species embedded within an inorganic matrix.

Class II which involves strong covalent chemical bonds between organic and inorganic compounds.

Both types of sol-gel have been prepared and studied by NLO. The doped gel (class I) was prepared with nitrocalix[4]arene **1**. Hybrid sol-gel matrix with grafted chromophore was obtained by using the nitrocalix[4]arene **5** derivative as a dye.

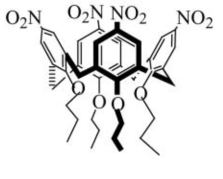

Fig. 1 Tetranitrotetrapropoxycalix[4]arene **1**.

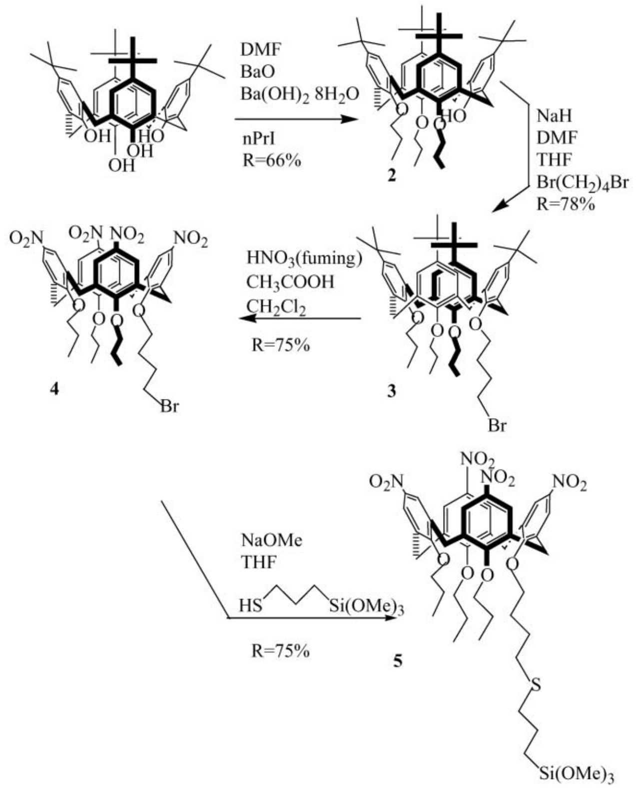

Fig. 2 Synthesis of 5,11,17,23-tetranitro-25-[4-[3-(trimethoxysilyl)propylthio]butyloxy]-26,27,28-tripropyloxycalix[4]arene **5**.

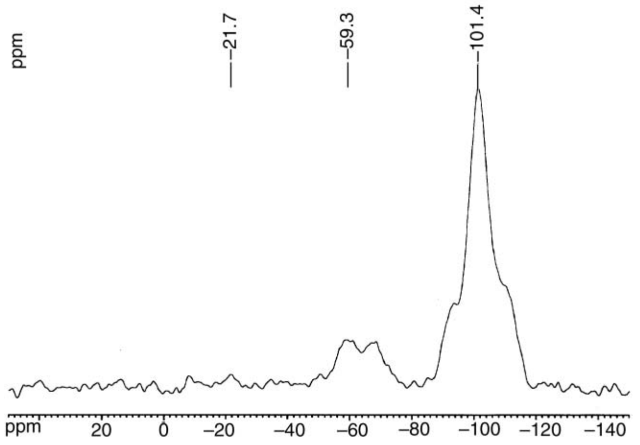

Fig. 3 ^{29}Si CP/MAS NMR spectrum of the nitrocalix[4]arene **5**–TEOS gel (class II).

The ^{29}Si CP/MAS NMR spectrum of the gel of the nitrocalix[4]arene **5**–TEOS is shown in Fig. 3. There are several signals[16] due to Q (tetrafunctional) and T (trifunctional) silicon–oxygen units (Table 1). The signals at −50, −60 and −70 ppm show that the nitrocalix[4]arene, **5**, was effectively covalently bound into the silica network. The ^{29}Si CP/MAS NMR spectrum of the doped gel (nitrocalixarene **1**–TEOS) is shown in Fig. 4. The signals corresponding to the Q silicon–oxygen units are present but no peaks corresponding to the directly bonded Si–C atoms are observed. Comparing spectra in Fig. 3 and Fig. 4, one can see that the signal of siloxane is the most important one, this illustrating the formation of a basic silica gel.

Table 1 Chemical shifts of most important peaks in ^{29}Si CP/MAS NMR spectra of gels of class I and class II

Peaks	δ (ppm) Class I	δ (ppm) Class II
$Si(OSi)_4$	−108.6	−110
$Si(OSi)_3(OH)$	−101	−101.4
$Si(OSi)_2(OH)_2$	−92	−94
$Si(C)(OSi)_3$		−70
$Si(C)(OSi)_2(OH)$		−60
$Si(C)(OSi)_2(OH)_2$		−50

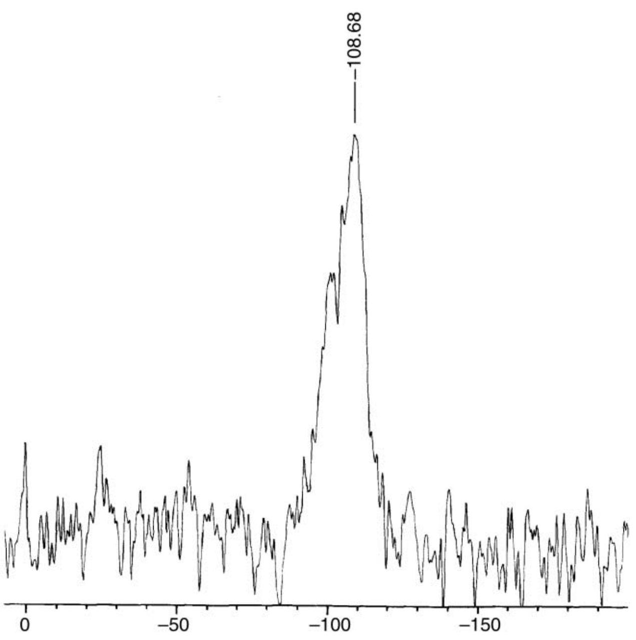

Fig. 4 ^{29}Si CP/MAS NMR spectrum of the nitrocalix[4]arene **1**–TEOS gel (class I).

Contact mode AFM images for both classes of sol-gel were obtained. In Fig. 5a, 5b, and 5c are given topographic images, at 10 µm scan range, of the class I systems containing respectively at 240, 120 and 80 TiO_2 : calixarene molar ratios; the area analysis results, along with diameter, height, and particle density, are given in Table 2.

As can be clearly seen, there exists an apparent phase separation in the class I films (this is confirmed by the friction force and force modulation images). The objects observed have diameters of 0.7, 0.6 and 0.5 µm for increasing calixarene concentrations, with the heights averaging 50 nm. The density of objects increases from 28/100 µm^2 to 40/100 µm^2 and finally to 130/100 µm^2 as titania : calixarene molar ratios decrease from 80 through 120 to 240. In view of this, we believe that the observed objects are composed mainly of the calixarenes, which have dephased from the solid-gel matrix.

Fig. 6a and 6b present the topographic images of two class II sol-gels with calixarene : TEOS molar ratios 1 : 19 and 1 : 39 respectively; area analysis data are given in Table 3. For the higher calixarene concentrations, spherical and apparently empty objects are present; analysis of this system, after poling (Fig. 6c), shows no apparent changes in the structure of the sol-gel. The sample 1 : 19 appears to be of a much more homogenous nature with a grainy structure.

Differences have been observed between the two types of films in m-line spectroscopy. Class II films have been studied at 543.5 nm (see below). They support two modes of each polarisation and their refractive index is 1.505 (± 0.001). Surprisingly the class II film thickness is dependent on the nature of the substrate even when the substrates have been cleaned using the same procedure. The materials were obtained in a two-step deposition process. Class II film thicknesses are 1.482 (± 0.006) µm, for two depositions, and 1.615 (± 0.006) µm for films deposited onto silica and Pyrex respectively.

Unfortunately TiO_2 class I films support only one mode of each polarisation. They are much thinner (around 140 nm thick) than the class II films and exhibit a refractive index

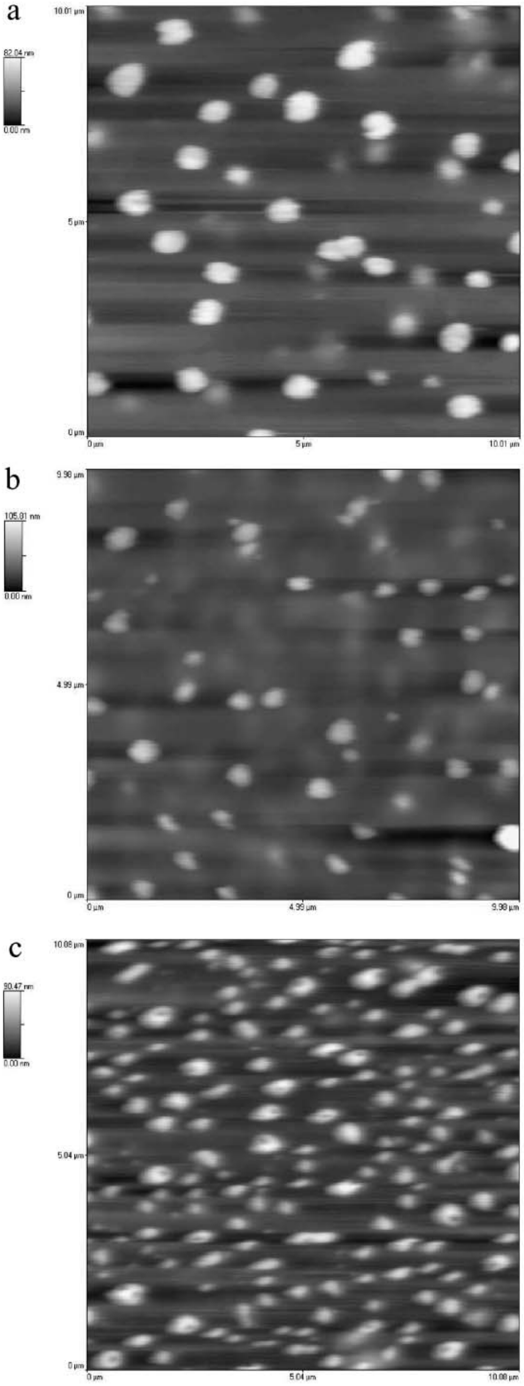

Fig. 5 AFM topographic contact mode images, at 10 µm scan range, of the class I systems containing respectively at 240, 120 and 80 molar ratios TiO_2-calixarenes.

around 1.82, not far from pure sol-gel TiO_2 films prepared under similar conditions.[17] This undoubtedly arises from the the low quantity of calixarene within the TiO_2 sol-gel.

Table 2 AFM area and particle analysis of class I sol-gel systems; diameter and height values are the average of 25 measurements in the line analysis module of the SPML 5.0 software package

Titania : calixarene molar ratio	240	120	80
Average diameter/µm	0.7 ± 0.1	0.6 ± 0.1	0.5 ± 0.1
Average height/nm	52 ± 10	46 ± 7	52 ± 10
Maximum height/nm	103.5	213.9	108.87
Roughness (RMS)/nm	15.5	18.7	16.4
Roughness (Ra)/nm	10.5	14.2	12.2
Particle density (/100 μm^2)	28	40	130

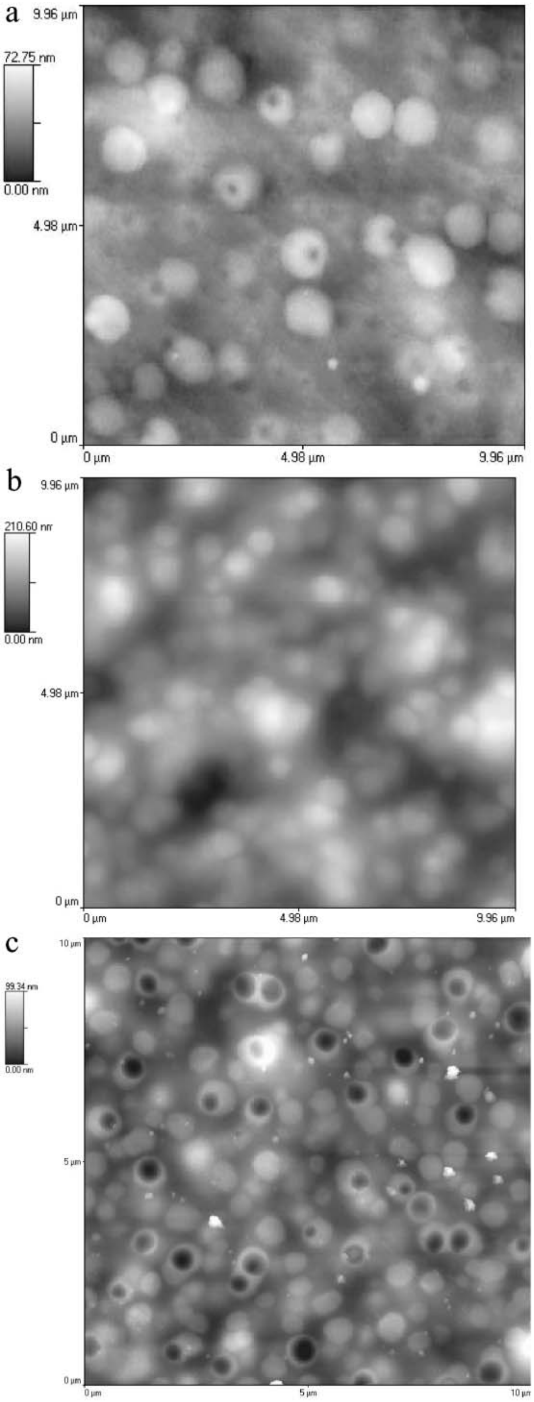

Fig. 6 Topographic images of class II calixarene sol-gels prior to poling [(a) and (b)] and topographic image of the class II sol-gel shown in (a) after poling (c); all images are 10 µm scan range.

The two types of films have been studied for their NLO properties. Corona poling was used to induce the non-centrosymmetry needed for macroscopic second-order non linearities. The best results were obtained when the samples were heated at 120 °C during the poling. For films of doped gel *i.e.* Class I, no NLO response was detected. It seems that

Table 3 Area analysis of class II sol-gel systems, measurements derived from the area analysis mode of the SPML 5.0 software package

Calixarene : TEOS molar ratio	Ra/nm	RMS/nm	Maximum height/nm
1 : 19	24.4	30.4	270
1 : 39	8.5	32.3	82

in this case the orientation of the calixarene molecules within the matrix must relax extremely rapidly; this is not unexpected as the unbound molecules are free to move within the matrix. On the other hand, organic–inorganic hybrid films in which the chromophore nitrocalix[4]arene **5** was covalently bound into the silica network, exhibited a high NLO response (d_{33}) that remained constant immediately after poling. We measured for d_{33} a value of 7.2 pm V^{-1} for a 0.79 μm thick film (nitrocalix[4]arene **5**–tetraethoxysilane 1 : 19 molar ratio) at 1064 nm. The same value was measured 15 days after poling. After two months, the d_{33} value had decreased by only 20% at room temperature. Reinhoudt described thin film NLO properties of doped polymer of nitrocalix[4]arene **1** in poly(methyl methacrylate).[18] The best result in these experiments was a d_{33} value of 7.2 pm V^{-1} with a poling neat film. In contrast to our results, they observed 10 days later an important (65%) decrease of the initial d_{33} values. These results underline the interest of grafted material.

4 Conclusions

This work presents the first direct elaboration of calixarene sol-gel matrix for NLO. The obtained materials were characterized by ^{29}Si NMR. There was no detectable NLO response for doped gel. On the contrary, thin films of calixarene grafted sol-gel exhibited high and temporally stable NLO responses.

Acknowledgement

This work has been supported by the French "Centre National de la Recherche Scientifique" *via* the Groupement de Recherche "Matériaux et Fonctions de l'Optique Non Linére". One of us (M. R.) thanks EZUS Lyon I for a grant. We thank also Dr F. Lefebvre for some experiments.

References

1 P. Prasad and D. J. Williams, in *Introduction to Nonlinear Optical Effects in Molecules and Polymers*, Wiley, New York, 1991.
2 D. S. Chemla and J. Zyss, in *Nonlinear Optical Properties of Organic Molecules and Crystals*, Academic Press, New York, 1987.
3 J. D. Mackenzie and D. R. Ulrich, *SPIE*, 1990, **2**, 1328; F. Chaput, D. Riehl, Y. Levy and J. P. Boilot, *Chem. Mater.*, 1993, **5**(5), 589; C. Sanchez and B. Lebeau, *Pure Appl. Opt.*, 1996, **5**, 689.
4 D. Riehl, F. Chaput, A. Roustamian, Y. Levy and J. P. Boilot, *Nonlinear Opt.*, 1995, **9**, 305.
5 C. D. Gutsche, in *Calixarenes Revisited*, Royal Society of Chemistry, Cambridge, 1998.
6 E. Kelderman, L. Derhaeg, G. J. Heesink, W. Verboom, J. F. Engbersen, N. F. van Hulst, A. Persoons and D. N. Reinhoudt, *Angew. Chem., Int. Ed. Engl.*, 1992, **31**(8), 1075; E. Kelderman, L. Derhaeg, G. J. Heesink, W. Verboom, J. F. Engbersen, S. Harkema, A. Persoons and D. N. Reinhoudt, *Supramol. Chem.*, 1993, **2**, 183; G. J. Heesink, N. F. van Hulst, B. Bölger, E. Kelderman, J. F. Engbersen, W. Verboom and D. N. Reinhoudt, *Appl. Phys. Lett.*, 1993, **62**(17), 2015.
7 P. J. Kenis, O. F. Noordman, N. F. Van Hulst, J. F. Engbersen, D. N. Reinhoudt, B. H. Hams and C. J. van der Vorst, *Chem. Mater.*, 1997, **9**, 596.
8 W. Verboom, A. Durie, R. J. Egberink, Z. Asfari and D. N. Reinhoudt, *J. Org. Chem.*, 1992, **57**, 1313.
9 K. Wamoto, K. Araki and S. Shinkai, *J. Org. Chem.*, 1991, **56**(16), 4955.
10 C. Urlacher, *PhD Thesis*, Lyon, 1996.
11 M. Ulrich and R. Torge, *Appl. Opt.*, 1973, **12**, 2901.
12 J. L. Oudar, *J. Chem. Phys.*, 1977, **67**, 446.
13 T. Thami, P. Bassoul, M. A. Petit, J. Simon, A. Fort, M. Barzoukas and A. Villaeys, *J. Am. Chem. Soc.*, 1992, **114**, 915.
14 J. Jerphagnon and S. K. Kurtz, *J. Appl. Phys.*, 1970, **41**, 1667.
15 P. Judeinstein and C. Sanchez, *J. Mater. Chem.*, 1996, **6**(4), 511.
16 X. Z. Xiao, Y. Q. Feng, S. L. Da and Y. Zhang, *Chromatographia*, 1999, 643.
17 M. Bahtat, *PhD Thesis*, Lyon, 1996.
18 E. Kelderman, G. J. Heesink, L. Derhaeg, T. Verbiest, P. T. Klaase, W. Verboom, J. F. Engbersen, N. F. van Hulst, K. Clays, A. Persoons and D. N. Reinhoudt, *Adv. Mater.*, 1993, **5**(12), 925.